有机化学 DOI: 10.6023/cjoc201712004 研究论文
Chinese Journal of Organic Chemistry ARTICLE

一种在含水介质和食物样品中快速和高灵敏度的双通道检测氰根的化学传感器

曲文娟 李文婷 张海丽 张有明*
林 奇 姚 虹 魏太保*
(西北师范大学化学化工学院 生态环境相关高分子材料教育部重点实验室 甘肃省高分子材料重点实验室 兰州 730070)

摘要 众所周知, 氰根离子(CN^-)是最具有毒性的阴离子之一, 它能够对环境和生物体造成很多不良的影响, 因此, 研究氰根离子的检测方法是非常有必要的, 尤其是在水中以及食物中进行检测. 然而, 由于游离态的氰根离子半衰期短, 但很多氰根离子检测方法所需分析时间较长并且容易受到其他阴离子的干扰, 这些都成为精确检测氰根离子的挑战. 利用氰根离子特殊的亲核性, 合成了一个基于萘并呋喃酰氯和 2-氨基苯并咪唑的新型传感器分子 **Q1-2**, 其设计原理在于通过调节分子内的氢键来影响分子的 π-共轭效应. 当加入氰根离子之后, 传感器 **Q1-2** 的紫外光谱出现红移现象, 并且荧光也立刻猝灭. 计算得到该传感器通过紫外和荧光检测氰根离子的最低检测限分别为 8.0769×10^{-7} 和 1.0510×10^{-9} mol/L. 其他共存的阴离子几乎不能干扰该识别过程. 不仅如此, **Q1-2** 可成功地应用于可见光和 365 nm 紫外灯照射下, 肉眼识别食物样品中和硅胶板上的氰根.

关键词 双通道检测; 氰根; 食物样品; 硅胶板

Rapid and Highly Sensitive Dual-Channel Detection of Cyanide in Aqueous Medium and the Applications in Food Samples

Qu, Wenjuan Li, Wenting Zhang, Haili Zhang, Youming*
Lin, Qi Yao, Hong Wei, Taibao*
(*Key Laboratory of Eco-Environment-Related Polymer Materials*, *Ministry of Education*, *Key Laboratory of Polymer Materials of Gansu Province*, *Northwest Normal University*, *Lanzhou 730070*)

Abstract It is well-known that cyanide anion (CN^-) is a hypertoxic anion, which can cause adverse effects in both environment and living beings. Thus, it is highly desirable to develop strategies for detecting cyanide, especially in aqueous medium and food. However, due to the short half-life of free cyanide, long analysis time and interference from other competitive anions are general challenges for accurate monitoring of cyanide. Taking advantage of the special nucleophilicity of cyanide, a new colorimetric and fluorescent sensor (**Q1-2**) was synthesized based on naphtho[2,1-*b*]furan-2-carbonyl chloride and 2-aminobenzimidazole which designed by tuning the intramolecular hydrogen bonding to affect the π-conjugated efficiency. Upon the addition of cyanide anion, the probe displayed a red-shift in absorption spectra and the fluorescence decreased immediately with the detection limit of 8.0769×10^{-7} and 1.0510×10^{-9} mol/L, respectively. Other anions gave nearly no interference. Furthermore, **Q1-2** was successfully applied to the naked eye identification for cyanide in the visible light and under the UV lamp in food samples and silica gel plates.

Keywords dual-channel detection; cyanide; food sample; silica gel plate

1 Introduction

The process of efficient fluorescent materials is of great interest in areas of supramolecular chemistry, such as imaging agents and sensors, components of light-emitting diodes, and data recording and storage.[1~8] Serve as an

* Corresponding authors. E-mail: weitaibao@126.com; zhangnwnu@126.com
Received December 3, 2017; revised March 3, 2018; published online March 16, 2018.
Project supported by the National Natural Science Foundation of China (Nos. 21662031, 21661028, 21574104, 21262032).
国家自然科学基金(Nos. 21662031, 21661028, 21574104, 21262032)资助项目.

important role in supramolecular chemistry, host-guest interaction study has caused an extensive concern of chemists in recent years.[9~13] Molecular recognition and sensing of anions are major concern because of the roles that anions play in a wide range of biological, environmental, and chemical processes.[14~17] Thus, the development of sensitive anion luminescence sensors continues to be an important field of research.[18~20] Various anions have their different roles and importance. Cyanide is widespread in industrial processes, such as gold mining, metallurgy, electroplating, and the synthesis of fibers and resins,[21,22] thus, inevitably causing accidental release of cyanide into the environment. The maximum permissive level of cyanide in drinking water is therefore set at 1.9 μmol/L by the World Health Organization (WHO).[23] Due to the great efforts made by the supramolecular scientists, numerous colorimetric and ratiometric cyanide sensors with sensitive and selective detection properties have been developed to date.[24~27] However, the reports concerning the applications in biological and environmental systems for cyanide were still very scarce.[28] Moreover, because cyanide anion is generally present in the aqueous medium in many biological and environmental systems, cyanide sensor which can commonly work in the aqueous medium is given priority. Therefore, the design and synthesis of cyanide sensors that can work well in aqueous medium is badly needed.

Herein, inspired by the fact that highly selective and sensitive detection of cyanide can be achieved through the nucleophilicity of cyanide.[29~31] We designed and synthesized a novel compound (**Q1-2**) containing amide and imidazole units in its main chain as a highly selective and sensitive cyanide sensor (Schemes 1 and 2). Their anion binding properties were investigated by means of UV-vis, ESI-MS, IR and ^{1}H NMR spectroscopy, as well as naked eyes. The detection limits were determined to be 8.0769×10^{-7} mol/L in visible light and 1.0510×10^{-9} mol/L under the UV-light for cyanide. Furthermore, the

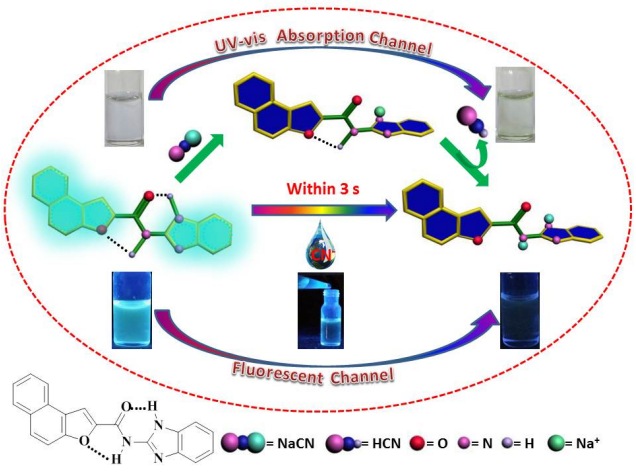

Scheme 1 Chemical structures and cartoon representations of **Q1-2** and cyanide in dimethyl sulfoxide (DMSO)/H_2O (V∶V=8∶2) solutions

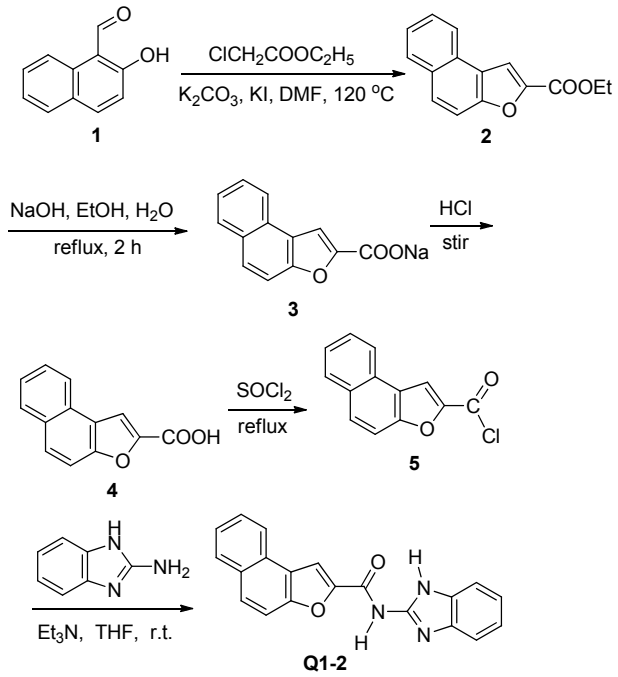

Scheme 2 Synthesis of the sensor molecule **Q1-2**

Q1-2 can be used to detect cyanide anion in food samples and the **Q1-2**-based silica gel plates were prepared which can be used to visually detect cyanide anion as a potential smart stimuli-responsive material in the field of supramolecular chemistry.

2 Results and discussion

The sensing properties of **Q1-2** were examined in DMSO/H_2O (V∶V=8∶2) hydroxyethylpiperazine ethane sulfonic acid (HEPES) solution through the addition of various anions (including F^-, Cl^-, Br^-, I^-, AcO^-, $H_2PO_4^-$, HSO_4^-, ClO_4^-, SCN^- and CN^-) (Figure 1). Upon the addition of 50 equiv. of various anions (except for cyanide anion), the absorption spectra of **Q1-2** did not show any significant change (Figure 1a). Nevertheless, in the presence of cyanide anion, an absorption bands red shift from 350 nm to 377 nm in the UV-visible spectrum, and there was accompanied by a visible color change from colorless to yellow, which could be clearly distinguished cyanide by the naked eyes. Upon the addition of 50 equiv. of various anions (except for cyanide anion), no substantial change observed in the emission spectra of **Q1-2**. The only significant response appeared when cyanide was added (Figure 1b), and a weak fluorescence was observed at about 485 nm and the band at 475 nm diminished. Emission spectra red shift mainly caused by the deprotonation of imidazole NH moiety, which lead to negative charge increased in sensor **Q1-2**, and electronic more beneficially transfer to fluorophore π*-system. Moreover, fluorescence quenching rate obtained according to fluorescence spectrum on the basis of $(F_o-F_c)/F_o$ (F_o: original fluorescence of fluorescent material; F_c: fluorescence after added quenching agent) was 62.94%. The color change from

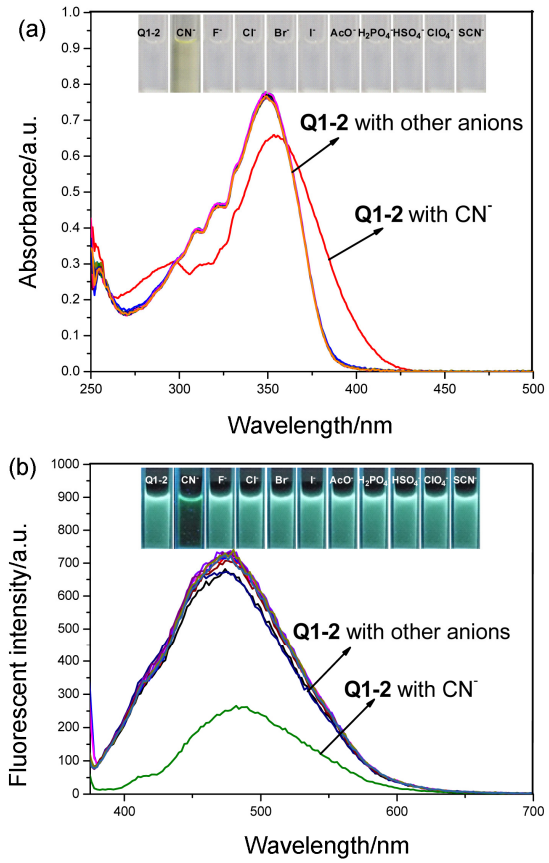

Figure 1 Absorbance spectra (a) and fluorescent spectra (b) of target compound **Q1-2** (20 μmol/L) in DMSO/H_2O (V∶V=8∶2) in the presence of cyanide and other anions (50 equiv.)
Inset: photograph showing the change in color of the solution of **Q1-2** in DMSO/H_2O (V∶V=8∶2, 20 μmol/L) after addition of cyanide and other anions at room temperature

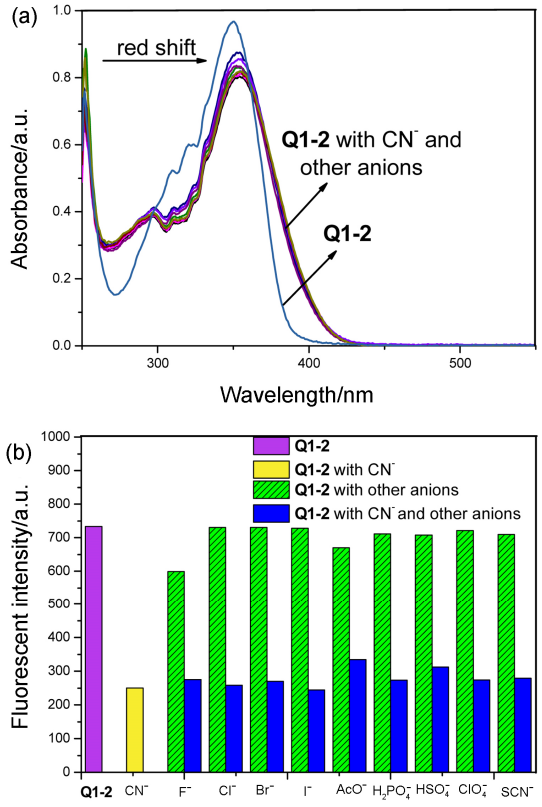

Figure 2 Absorbance data (a) and fluorescence emission data (b) for a 1∶50 mixture of **Q1-2** (20 μmol/L) and different tetrabutylammonium salts of anions in DMSO/H_2O (V∶V=8∶2) solutions at room temperature (excitation wavelength=365 nm)

blue-green to a quenched situation could be distinguished by the naked eyes under the UV-lamp. Thus, sensor **Q1-2** could be considered as a good ON-OFF cyanide fluorescent switch. The favourable selectivity, preferable detection system and dual-channel detect method of **Q1-2** was more remarkable than other systems reported in the literatures.

To further explore the utility of **Q1-2** as an anion-selective sensor for cyanide, competitive experiments were performed with 50 equiv. of cyanide and 50 equiv. of various other anions (F^-, Cl^-, Br^-, I^-, AcO^-, $H_2PO_4^-$, HSO_4^-, ClO_4^-, SCN^-) in a DMSO/H_2O (V∶V=8∶2) HEPES solution of **Q1-2**. The absorption spectrum of **Q1-2** with cyanide was not significantly influenced by the subsequent addition of competing anions (Figure 2a). Similarly, the obvious switching behavior was not affected even in the presence of all anions together (Figure 2b).

Furthermore, we also researched the sensing properties of **Q1-2** toward various cations (including Fe^{3+}, Hg^{2+}, Ag^+, Ca^{2+}, Cu^{2+}, Co^{2+}, Ni^{2+}, Cd^{2+}, Pb^{2+}, Zn^{2+}, Cr^{3+}, Mg^{2+}) in DMSO/H_2O (V∶V=8∶2) HEPES solution. Upon the addition of 20 equiv. of various cations, the absorption spectra and fluorescent spectra of **Q1-2** did not show any significant selectivity among these cations.

In order to investigate the optimized condition about the sensing behavior of **Q1-2** toward cyanide, the UV-vis absorption spectra and fluorescent spectra with different concentrations of cyanide were performed in DMSO/H_2O (V∶V=8∶2) HEPES solution of **Q1-2**. The incremental addition of cyanide (0～8 equiv.) to a DMSO/H_2O (V∶V=8∶2) HEPES solution of **Q1-2** (2×10^{-5} mol/L) at room temperature reveals a gradual decrease of the broad absorbance at 350 nm with a significant red shift. At the same time, a new broad band at 390 nm is also noted. This should be attributed to the deprotonation of N—H on imidazole and amide groups, which broke the large π-conjugation system between aminobenzimidazole and naphthofuran fluorophore in sensor molecule. However, no further change is observed in the absorption profile beyond the addition of 8 equiv. of cyanide (Figure 3).

Similarly, there is also an obvious variation in fluorescence spectrum during titrations with different concentrations of cyanide in **Q1-2** (2×10^{-5} mol/L) in DMSO/H_2O (V∶V=8∶2) solution. **Q1-2** exhibits a rather strong and broad emission profile with a maximum at 475 nm in DMSO/H_2O (V∶V=8∶2) solution. Nevertheless, the fluorescence emission spectral gradually decreased during titrations with different concentrations of cyanide from 0 to 12 equiv. As a consequence, the emission color changed from blue-green to a quenched situation in the presence of cyanide (Figure 4).

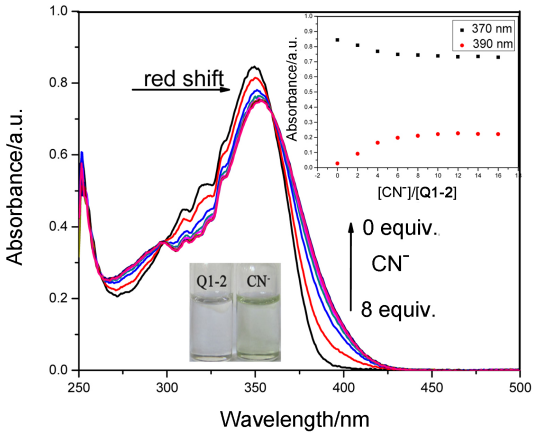

Figure 3 Absorption spectrum of **Q1-2** (20 μmol/L) in the presence of different concentration of cyanide in DMSO/H_2O (V∶V=8∶2) solutions at room temperature

Inset: A plot of absorbance intensity depending on the concentration of cyanide at 370 and 390 nm

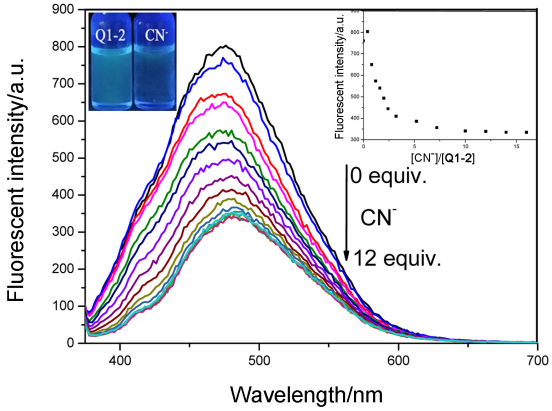

Figure 4 Fluorescent spectrum of **Q1-2** (20 μmol/L) in the presence of different concentration of cyanide in DMSO/H_2O (V∶V=8∶2) solutions at room temperature

Inset: A plot of fluorescent intensity depending on the concentration of cyanide at 475 nm (λ_{ex}=365 nm)

Furthermore, to determine the detection limit of **Q1-2**, the UV-Vis absorption spectral and the fluorescent spectrums of blank tests were measured 15 times and the standard deviation of the blank measurements was determined. The linear fitting were performed according to the titrations curves, and the mean intensity was calculated to determine the slope. The detection limit was calculated using the following equation:

Detection limit=3σ/S

Where σ is the standard deviation of the absorbance and emission intensity of **Q1-2** in the presence of cyanide and m is the slope between the absorbance and emission intensity and concentration.

The detection limits of UV-vis absorption spectral and the fluorescent spectrum were 8.0769×10^{-7} and 1.0510×10^{-9} mol/L for cyanide, respectively. This data can indicating that the probe can detect cyanide anion at very low concentrations in the environment.

Since the pH value affects the charge distribution of receptor **Q1-2** and may change its inherent fluorescence properties, the effect of various pH on the emission intensity of **Q1-2** in DMSO/H_2O (V∶V=8∶2) HEPES buffered solution was also studied. As shown in Figure 5, the **Q1-2**-CN^- showed significant fluorescence response in the range of pH 4～9. Meanwhile, with the increasing of pH, the receptor's fluorescent gradually decreased. These results indicate that **Q1-2** can detect CN^- in a range of pH from 4 to 9.

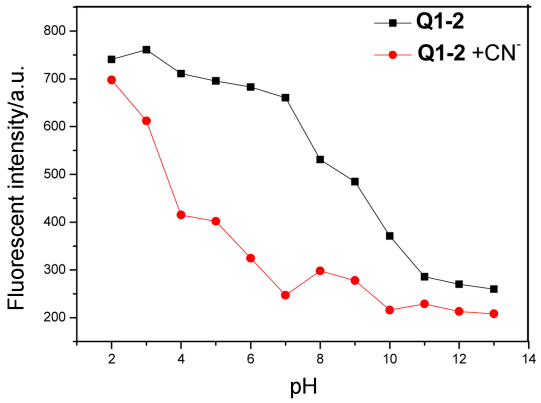

Figure 5 Effect of pH on the fluorescence spectra for **Q1-2** in response to CN^- (20 mol/L) from 2 to 13 in DMSO/H_2O (pH=7.0, V∶V=8∶2) solution (λ_{ex}=365 nm, λ_{em}=475 nm)

Subsequently, in detail, the recognition mechanism of the sensor **Q1-2** with cyanide was investigated by IR spectra, ESI/MS and ^{1}H NMR titration methods. The 1∶2 stoichiometry for **Q1-2** and NaCN was further confirmed by the appearance of a peak at m/z 372.01, assignable to [**Q1-2**+2Na^+−2H^+]+H^+ in the ESI/MS. The ESI/MS displayed a peak explain that the deprotonated **Q1-2** was coordinated with two sodium ions. IR spectrum of **Q1-2** shows two vibration band at 3387 and 3314 cm^{-1}, which can be assigned to stretching vibrational absorption peaks of amide NH and imidazole NH groups in the **Q1-2** molecule, respectively. The vibration band at 1630 cm^{-1} was attributed to the vibration of amide C=O. However, when **Q1-2** reacted with cyanide, the stretching vibration absorption peaks of amide NH and imidazole NH groups disappeared at 3387 and 3314 cm^{-1}, which indicated that **Q1-2** lost two H proton with the addition of cyanide (Figure 6).

The mechanism of **Q1-2** for cyanide sensing was further analyzed accordingly with ^{1}H NMR spectroscopy. Figure 7 shows the ^{1}H NMR of **Q1-2** upon the addition of cyanide in a DMSO-d_6 solution. Before addition of cyanide in **Q1-2**, the H proton signal peaks of amide NH and imidazole NH appeared at δ 12.64 at the same time. While after adding 0.1 equiv. of cyanide, the singles of amide NH and imidazole NH at δ 12.64 decreased and rapidly disappeared due to the deprotonation of sensor **Q1-2**. Also there were without any shift on the original aromatic protons, which was in accordance with previous studies that cyanide could taking the H proton away via deprotonating in the amide NH and imidazole NH moiety of **Q1-2** which broke the large π-conjugation system between ami-

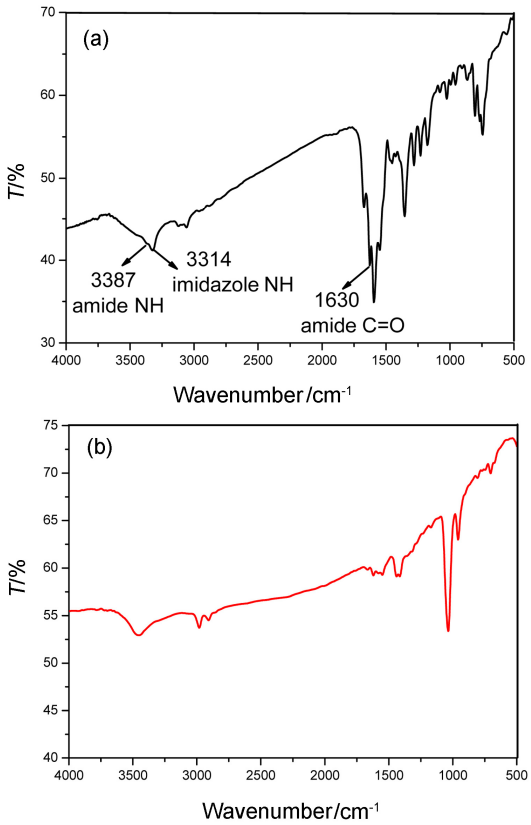

Figure 6 IR spectra of sensor **Q1-2** (a) and after adding cyanide anions (b) in KBr disks

nobenzimidazole and naphthofuran fluorophore in sensor molecule.

To further visually demonstrate the switching process of the fluorescence signal, a cartoon figure was drawn out in order to show the recognition mechanism. As shown in Figure 8, the strong fluorescence mainly due to the large

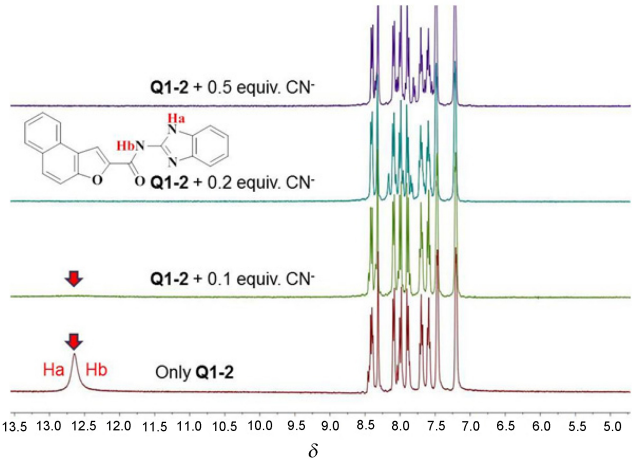

Figure 7 Partial ^{1}H NMR spectra of **Q1-2** (DMSO-d_6) and in the presence of varying amounts of cyanide anions (1 mol/L, D_2O)

intramolecular hydrogen bonding between imidazole and acyl group, together with that between amide and furan group in sensor molecule. On this account, this strong fluorescence is assigned to the large π-conjugation system caused by the aminobenzimidazole and naphthofuran fluorophore through intramolecular hydrogen bonding. Afterwards, with the addition of NaCN in the **Q1-2** solution, cyanide firstly took the H protons away from imidazole NH moiety and, which broke the intramolecular hydrogen bonding. Thereafter, the free sodium ion coordinated to the negatively charged N atom. After that, another cyanide interaction with amide NH, which further damaged the intramolecular hydrogen bonding and caused the free rotation of the sensor molecular. Then the free sodium ion coordinated to the negatively charged N atom, which

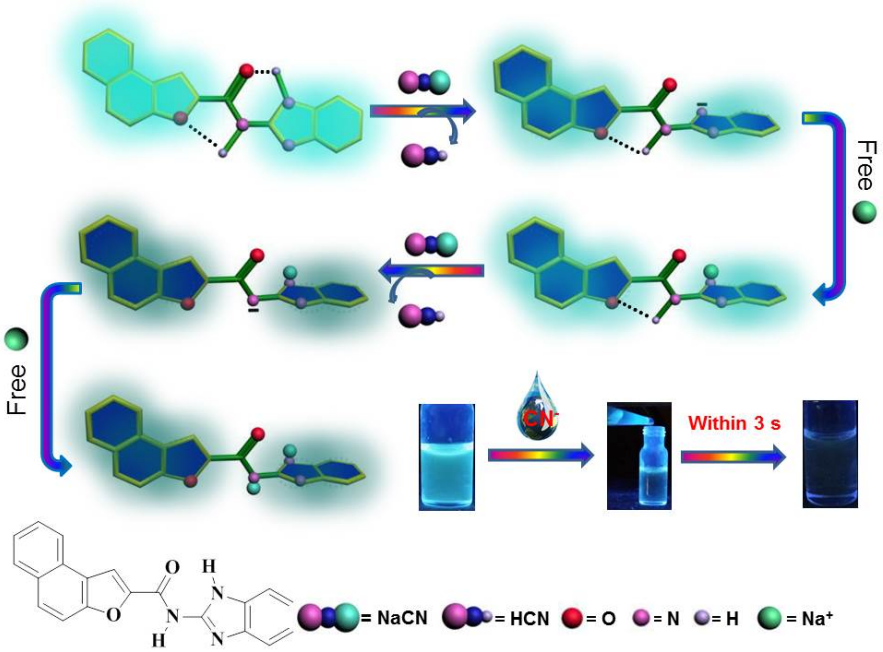

Figure 8 Proposed reaction mechanism of sensor **Q1-2** with NaCN

destroyed the coplanar molecule. As a result, the fluorescent intensity decreased with the addition of NaCN.

For convenient use in an on-site visual screening analysis, silica gel plates test kits were prepared by silica gel plates into DMSO/H_2O (V∶V=8∶2) solutions of **Q1-2** (0.1 mol/L) and then dried in air. For instance, as shown in Figure 9 when we wrote by a brush containing cyanide aqueous solution on the silica gel plate which dipped in **Q1-2**, a pale yellow mark can be observed in visible light and a brilliant blue-green fluorescent image disappeared under the 365 nm UV-lamp.

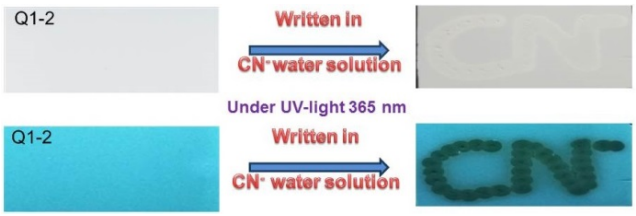

Figure 9 Photos of the silica gel plates utilized to sense cyanide in aqueous solution in visible light and under irradiation at 365 nm by a UV lamp

With the cyanide sensor in hand, we wondered if we can further use this sensor in daily life food samples. Bitter seed and cherry pit which usually contain cyanide anion in them were selected as the food samples. 100 g of bitter seeds was crushed and pulverized in mortar. Then, 300 mL of water and 0.5 g of NaOH were add into the sample and the obtained mixture was vigorously stirred for 15.0 min. The bitter seeds cyanide-containing solution (BSCS) was obtained by filtration. Furthermore, the cherry pit (100 g) was firstly mashed and soaked in 200 mL water and 100 mL NaOH (125 mmol/L) solution for 2 d. The mixture was then filtered to obtain the cherry pit cyanide-containing solution (SPCS). And then the sensor **Q1-2** was used to detect the cyanide anions in the two cyanide containing solutions. As shown in Figure 10 (b), after the addition of the cyanide solution BSCS or BSCS into the solution of **Q1-2** (20 μmol/L), the fluorescent emission intensity of the sensor **Q1-2** increased rapidly, providing the direct evidence for the detection of cyanide anions in the two different food samples. Furthermore, as shown in Figure 10 (a), the color changes from dim blue to blue-green could be distinguished by the naked eyes under the UV lamp (365 nm), which made the sensor **Q1-2** as a visual and convenient detection sensor for cyanide anions in food samples.

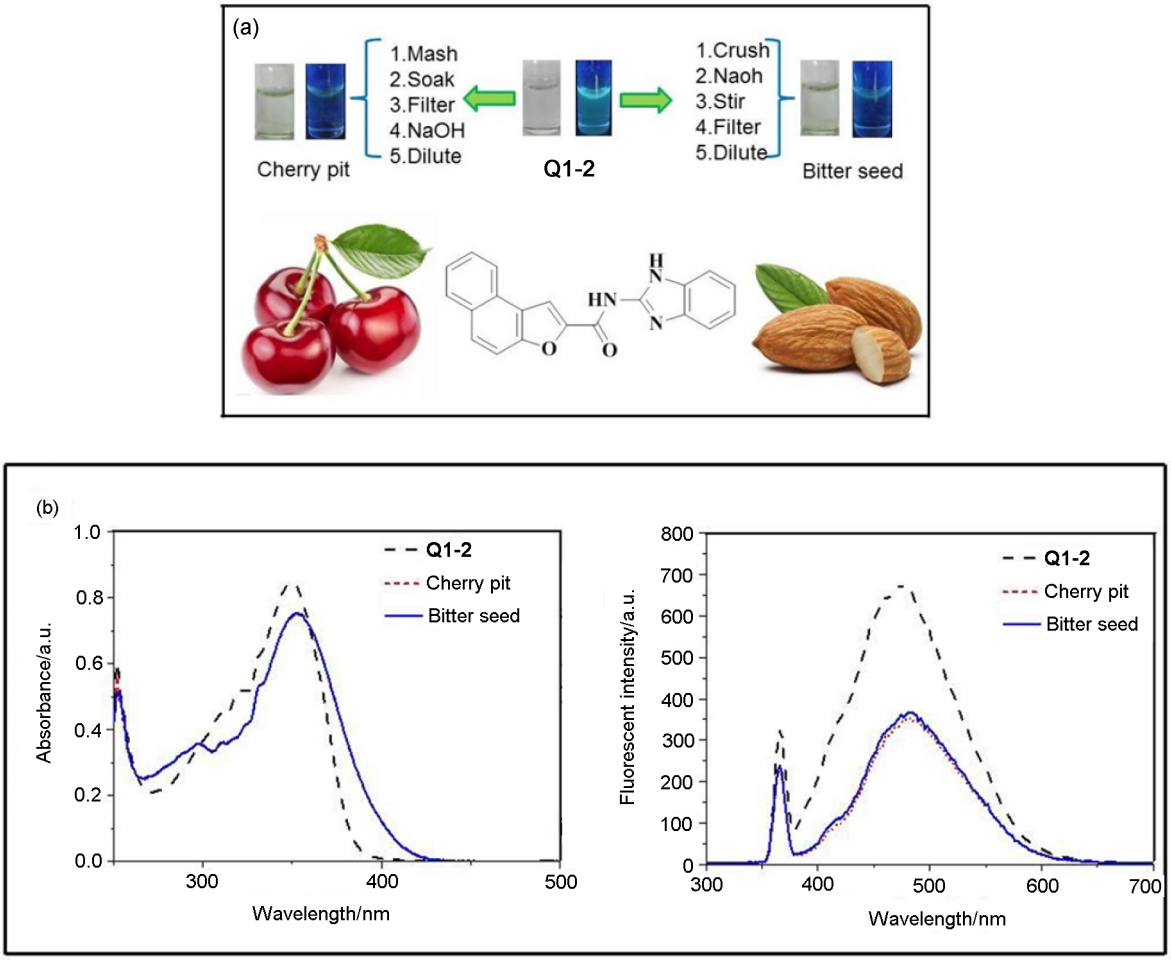

Figure 10 (a) Response photographs of **Q1-2** (20 μmol/L) in diluted bitter seeds and cherry pits filter and (b) UV-vis absorption spectral and fluorescence spectral response of **Q1-2** (20 μmol/L) in diluted bitter seeds and cherry pits filter

3 Conclusions

A new fluorescent and colorimetric sensor (**Q1-2**) toward cyanide was designed based on the interactions between cyanide to the amide NH and imidazole NH moiety. The sensor demonstrated some advantages such as good sensitivity and high selectivity for cyanide, low detection limits both in UV-vis absorption spectral and the fluorescent spectrum in DMSO/H_2O (V∶V=8∶2) solution, relative good solubility in aqueous media, rapid naked-eyes response (within 3 s), as well as the successful application in silica gel plates and food samples. The design approach in this work provided some useful information for the development of optical sensors, and suggesting a potential high efficiency application in natural environment.

4 Experimental section

4.1 Materials and physical methods

^{1}H NMR and ^{13}C NMR spectra were recorded on an Agilent DD2 at 600 MHz spectra. ^{1}H chemical shifts are reported in ppm downfield from tetramethylsilane (TMS, δ scale) with the solvent resonances as internal standards). UV-visible spectra were recorded on a Shimadzu UV-2550 spectrometer. Photoluminescence spectra were performed on a Shimadzu RF-5301 fluorescence spectrophotometer. Melting points were measured on an X-4 digital melting-point apparatus. The infrared spectra were performed on a Digilab FTS-3000 FT-IR spectrophotometer.

Fresh double distilled water was used throughout the experiment. All other reagents and solvents were commercially available at analytical grade and were used without further purification.

4.2 Synthesis of sensor molecule *N*-(1*H*-benzo[*d*]-imidazol-2-yl)naphtho[2,1-*b*]furan-2-carboxamide (Q1-2)

Compound **Q1-2** can be readily prepared by a simple and low-cost amide reaction of naphtha[2,1-*b*]furan-2-carbonyl chloride and 2-aminobenzimidazole (Scheme 2). The synthesis of naphtha[2,1-*b*]furan-2-carbonyl chloride can be found in the reported literature.[32] naphtha[2,1-*b*]furan-2-carbonyl chloride (0.462 g, 2 mmol), 2-aminobenzimidazole (0.333 g, 2.5 mmol) and 2.5 mL of triethylamine (Et_3N) were combined in hot absolute tetrahydrofuran (THF, 30 mL). The solution was stirred under reflux for 6 h. After cooling to room temperature, the yellow precipitate was filtered, washed three times with hot absolute tetrahydrofuran, then recrystallized with THF to give a yellow powder product **Q1-2** (1.53 mmol) in 76.5% yield. m.p.＞300 ℃; IR (KBr) v: 3387 (amide NH), 3314 (imidazole NH), 3120 (C═CH), 3060 (ArH), 1630 (C═O), 1596 (C═C) cm^{-1}; ^{1}H NMR (DMSO-d_6, 600 MHz) δ: 12.64 (s, 2H, imidazole NH and amide NH), 7.20～8.42 (m, 11H, ArH); ^{13}C NMR (DMSO-d_6, 150 MHz) δ: 162.70, 160.45, 153.08, 151.48, 131.91, 130.39, 129.12, 128.22, 127.96, 127.70, 127.44, 125.84, 125.49, 123.95, 123.24, 122.56, 113.40, 113.05, 112.65, 110.12. ESI-MS m/z: 328.10 [M＋H$^+$]. Anal. calcd for $C_{20}H_{13}N_3O_2$: C 73.39, H 3.97, N 12.84; found C 73.32, H 3.99, N 12.85.

4.3 General procedure for UV-vis experiments

All the UV-vis experiments were carried out in DMSO/H_2O (V∶V=8∶2) HEPES solution on a Shimadzu UV-2550 spectrometer. Any changes in the UV-vis spectra of the synthesized compound were recorded on addition of tetrabutylammonium salts while keeping the ligand concentration constant (2.0×10^{-5} mol/L) in all experiments. Tetrabutylammonium salt (1.0×10^{-3} mol/L) of anions (F^-, Cl^-, Br^-, I^-, AcO^-, $H_2PO_4^-$, HSO_4^-, and ClO_4^-) and sodium salt (1.0×10^{-3} mol/L) of anions (CN^- and SCN^-) were used for the UV-vis experiments.

4.4 General procedure for fluorescence spectra experiments

All the fluorescence spectroscopy was carried out in DMSO/H_2O (V∶V=8∶2) HEPES solution on a Shimadzu RF-5301 spectrometer. Any changes in the fluorescence spectra of the synthesized compound were recorded on addition of tetrabutylammonium salts while keeping the ligand concentration constant (2.0×10^{-5} mol/L) in all experiments. Tetrabutylammonium salt (1.0×10^{-3} mol/L) of anions (F^-, Cl^-, Br^-, I^-, AcO^-, $H_2PO_4^-$, HSO_4^- and ClO_4^-) and sodium salt (1.0×10 mol/L^{-3} mol/L) of anions (CN^- and SCN^-) were used for the fluorescence experiments

4.5 General procedure for ^{1}H NMR experiments

For ^{1}H NMR titrations, the solution of **Q1-2** was prepared in DMSO-d_6 and the appropriate concentrated solution of guest was prepared in deuterium water. Aliquots of the two solutions were mixed directly in NMR tubes.

Supporting Information ^{1}H NMR and ^{13}C NMR spectra for **Q1-2**, ESI/MS of **Q1-2** and **Q1-2** with NaCN, and the determine of the UV-Vis and fluorescent detection limit for cyanide. The Supporting Information is available free of charge via the Internet at http://sioc- journal.cn/.

References

[1] Yan, X. Z.; Wang, M.; Cook, T. R.; Zhang, M. M.; Saha, M. L.; Zhou, Z. X.; Li, X. P.; Huang, F. H.; Stang, P. J. *J. Am. Chem. Soc.* **2016**, *138*, 4580.

[2] Shi, B. B.; Jie, K. C.; Zhou, Y. J.; Zhou, J.; Xia, D. Y.; Huang, F. H. *J. Am. Chem. Soc.* **2016**, *138*, 80.

[3] Shi, B. B.; Jie, K. C.; Zhou, Y. J.; Xia, D. Y.; Yao, Y. *Chem. Commun.* **2015**, *51*, 4503.

[4] Wang, S.; Fei, X.; Guo, J.; Yang, Q.; Li, Y.; Song, Y. *Talanta* **2016**, *148*, 229.

[5] Yao, Y.; Jie, K.; Zhou, Y.; Xue, M. *Tetrahedron Lett.* **2014**, *55*, 3195.

[6] Sun, Y.; Hu, J. H.; Qi, J.; Li, J. B. *Spectrochim. Acta Part A*: *Mol. Biomol. Spectrosc.* **2016**, *167*, 101.

[7] Yu, M.; Liu, Y.; Chen, Y.; Zhang, N.; Liu, Y. *Chin. J. Chem.* **2012**, *30*, 1948.

[8] Zhang, Z.; Wang, H.; Zhang, H.; Liu, Y. *Chin. J. Chem.* **2013**, *31*, 598.

[9] Wang, L.; Zhu, L.; Li, L.; Cao, D. *RSC Adv.* **2016**, *6*, 55182.

[10] Wang, L.; Du, J.; Cao, D. *Sens. Actuators*, *B* **2014**, *198*, 455.
[11] Chen, L. J.; Ren, Y. Y.; Wu, N. W.; Sun, B.; Ma, J. Q.; Zhang, L.; Tan, H. W.; Liu, M. H.; Li, X. P.; Yang, H. B. *J. Am. Chem. Soc.* **2015**, *137*, 11725.
[12] Liu, T.; Huo, F.; Li, J.; Cheng, F.; Yin, C. *Sens. Actuators*, *B* **2017**, *239*, 526.
[13] Wang, Q.; Cheng, M.; Cao, Y. H.; Qiang, J. L.; Wang, L. Y. *Acta Chim. Sinica* **2016**, *74*, 9 (in Chinese).
(王其, 程明, 曹逸涵, 强琚莉, 王乐勇, 化学学报, **2016**, *74*, 9.)
[14] Gale, P. A. *Chem. Soc. Rev*. **2010**, *39*, 3746.
[15] Gale, P. A. *Chem. Commun*. **2011**, *47*, 82.
[16] Erdemir, S.; Kocyigit, O.; Alici, O.; Malkondu, S. *Tetrahedron Lett*. **2013**, *54*, 613.
[17] Singh, Y.; Ghosh, T. *Talanta* **2016**, *148*, 257.
[18] Fillaut, J. L.; Akdas-Kilig, H.; Dean, E.; Latouche, C.; Boucekkine, A. *Inorg. Chem*. **2013**, *52*, 4890.
[19] Huang, Q.; Qu, W. J.; Chen, J.; Lin, Q.; Yao, H.; Zhang, Y. M.; Wei, T. B. *Chin. J. Org. Chem*. **2017**, *37*, 629 (in Chinese).
(黄青, 曲文娟, 陈洁, 林奇, 姚虹, 张有明, 魏太保, 有机化学, **2017**, *37*, 629.)
[20] Li, W. T.; Qu, W. J.; Zhang, H. L.; Li, X.; Lin, Q.; Yao, H.; Zhang, Y. M.; Wei, T. B. *Chin. J. Org. Chem*. **2017**, *37*, 2619 (in Chinese).
(李文婷, 曲文娟, 张海丽, 李翔, 林奇, 姚虹, 张有明, 魏太保, 有机化学, **2017**, *37*, 2619.)
[21] Kumari, N.; Jha, S.; Bhattacharya, S. *J. Org. Chem*. **2011**, *76*, 8215.
[22] Lin, W. C.; Fang, S. K.; Hu, J. W.; Tsai, H. Y.; Chen, K. Y. *Anal. Chem*. **2014**, *86*, 4648.
[23] Shiraishi, Y.; Nakamura, M.; Hayashi, N.; Hirai, T. *Anal. Chem*. **2016**, *88*, 6805.
[24] Kim, H. J.; Ko, K. C.; Lee, J. H.; Lee, J. Y.; Kim, J. S. *Chem. Commun*. **2011**, *47*, 2886.
[25] Wang, L.; Li, L.; Cao, D. *Sens. Actuators*, *B* **2016**, *228*, 347.
[26] Chen, X.; Zhou, Y.; Peng, X.; Yoon, J. *Chem. Soc. Rev*. **2010**, *39*, 2120.
[27] Xu, Z.; Kim, S. K.; Yoon, J. *Chem. Soc. Rev*. **2010**, *39*, 1457.
[28] Cheng, X.; Tang, R.; Jia, H.; Feng, J.; Qin, J.; Li, Z. *ACS Appl. Mater. Interfaces* **2012**, *4*, 4387.
[29] Wu, X.; Xu, B.; Tong, H.; Wang, L. *Macromolecules* **2011**, *44*, 4241.
[30] Li, J.; Qi, X.; Wei, W.; Liu, Y.; Xu, X.; Lin, Q.; Dong, W. *Sens. Actuators*, *B* **2015**, *220*, 986.
[31] Li, J.; Qi, X.; Wei, W.; Zuo, G.; Dong, W. *Sens. Actuators*, *B* **2016**, *232*, 666.
[32] Qu, W. J.; Guan, J.; Wei, T. B.; Yan, G. T.; Lin, Q.; Zhang, Y. M. *RSC Adv*. **2016**, *6*, 35804.

(Cheng, F.)

